

Dependence of stimulated Brillouin scattering on laser intensity, laser f number, and ion species in hohlraum plasmas

Juan C. Fernández,¹ J. A. Cobble,¹ B. H. Failor,² W. W. Hsing,¹ H. A. Rose,¹
B. H. Wilde,¹ K. S. Bradley,^{1,*}

P. L. Gobby,¹ R. Kirkwood,³ H. N. Kornblum,³ D. S. Montgomery,³ and M. D. Wilke¹

¹Los Alamos National Laboratory, Los Alamos, New Mexico 87545

²Lawrence Livermore National Laboratory, Livermore, California 94550

³Physics International, San Leandro, California 94577

(Received 23 January 1995; revised manuscript received 1 August 1995)

Stimulated Brillouin scattering has been studied in plasma conditions approaching those expected within laser-driven cavities (hohlraums) capable of driving a fusion capsule to ignition with x rays. These conditions are achieved using a gas-filled hohlraum design that was fielded at the Nova laser. As the intensity of an interaction beam (351 nm in wavelength) is increased above an onset value I_c , the measured Brillouin backscatter into the lens rises sharply and saturates. I_c decreases as the optic f number increases. The saturation level depends on the gas ion species.

PACS number(s): 52.35.Nx, 52.35.Mw, 52.40.Nk, 52.50.Jm

I. INTRODUCTION

Control of laser-plasma instability is crucial for success in indirect-drive laser fusion [1], where the x rays within a case (called a hohlraum) implode a fusion capsule. Ignition hohlraums, such as those planned for the National Ignition Facility (NIF) [2], will be filled with millimeter size underdense plasmas with low- Z (low ionization state) ions [3]. This plasma (provided by a gas fill or a liner) resists encroachment by the high- Z wall into the hohlraum volume while allowing propagation of the laser to the high- Z plasma, where conversion to x rays occurs. In particular, NIF beams will traverse a 2–3 mm path where the electron and ion temperatures are $T_e = 3\text{--}5$ keV, $T_i/T_e \approx 0.5$, and the electron density is $n_e/n_c \approx 0.1$ during peak laser power [4]. ($n_c = 9 \times 10^{21}$ cm⁻³ is the critical density above which $\lambda = 351$ nm laser light cannot propagate.) In these plasmas, stimulated Brillouin scattering (SBS) [5] could be significant, particularly backscatter, which is expected to have the highest gain.

SBS levels of 351-nm lasers in supersonic, underdense CH plasmas are low (< 5%) [6,7], contrary to the case of 1053-nm lasers [8]. But these encouraging single-beam experiments lacked quantitative theoretical understanding. They did not have the laser energy, beam smoothing, or the geometry necessary to achieve simultaneously conditions in which the SBS threat in ignition hohlraums could be assessed confidently.

Nova experiments (contemporary with those reported herein) with gas-filled bags of polyimide (C₂₂H₁₀O₅N₂) skin with sub- μ m thickness come closer to achieving the desired conditions [4,9]. However, in order to extrapolate to ignition conditions, it is also important to study Brillouin backscatter in the relatively complex hohlraum plasmas. The wide range of densities, temperatures, Z ,

and gradient lengths in such a system potentially allows the coexistence of various instabilities that could either seed [7] or compete [10,11] with each other. Previous measurements of SBS of 527-nm beams in hohlraums [12] lacked the scale lengths and the low- Z plasma fill characteristic of present ignition-hohlraum designs. SBS studies on Nova (complementary and contemporary to ours) with an alternative long-scale-length hohlraum design [13] have compared SBS levels to linear-theory predictions within a limited range of relatively high intensities using a single hydrocarbon gas fill.

This paper presents the first study of the dependence of SBS of 351-nm light on laser intensity, optic f number and ion mixtures in well-characterized hohlraums containing plasmas approaching NIF plasma scale lengths and conditions. These plasmas are produced by the Nova laser [14] despite its much lower energy relative to NIF. We compare to predictions from a theoretical model, which accounts for the laser speckle pattern [15].

II. HOHLRAUM TARGETS

The Nova gas-filled gold hohlraum used in our study, pictured in Fig. 1 (left), is cylindrically symmetric with a length of 1.6 mm and a diameter of 3.2 mm. The round sections have a 0.7 mm radius of curvature. The two laser-entrance holes (LEH's) have a diameter of 1.6 mm. All beams cross the symmetry axis 0.7 mm from the hohlraum midplane, i.e., 0.1 mm inside their LEH.

Three gas fills at 1 atm. pressure are used: C₅H₁₂, C₅D₁₂, and CO₂, resulting in (n_e/n_c) = 0.12, 0.12, and 0.06, respectively, when fully ionized. Gas fills at 5 atm. of He and He-H (same number of atoms each) have also been used, resulting in $n_e/n_c = 0.03$. The hohlraum pressure is monitored until a few seconds before the shot. With 1 atm. pressure, silicon-nitride LEH windows (0.25- μ m thickness, 1.8-mm length and width, and 6-mm curvature radius when pressurized) keep the gas in the hohlraum. With 5 atm., polyimide windows (0.5- μ m thickness, and 1-mm curvature radius) are used. Window material strengths set the pressure limits.

*Present address: Lawrence Livermore National Lab, Livermore, CA 94550.

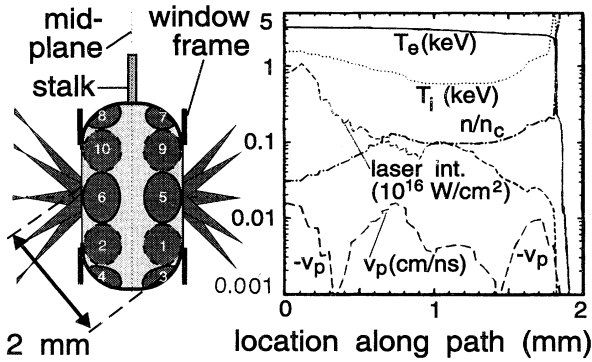


FIG. 1. Left: The gas-filled hohlraum is illustrated. The footprints of the ten Nova beams incident on the inner wall are indicated (those on the far wall have a dashed outline). Right: Calculated profiles within the hohlraum along a beam path (starting at the LEH) are plotted for time 1 ns.

Figure 1 (right) shows two-dimensional radiation hydrodynamic modeling (using the LASNEX computer code [16]) of T_e , T_i , n_e , laser intensity and fluid velocity v_p along the path of beam propagation (\hat{k}_0) in a hohlraum filled with regular or deuterated neopentane (C_5H_{12} or C_5D_{12}). LASNEX includes no scatter from parametric instabilities. In these experiments, nine $f/4.3$ beams turn on at time 0, reaching a power level of 2 TW each in less than 0.1 ns. Power linearly increases to 3 TW at time 1.4 ns, when the beams are turned off. These drive beams diverge for a distance of 3.4 mm from best focus before hitting the hohlraum wall. According to the simulation, the plasma conditions shown in Fig. 1 are approximately maintained for the last 0.5 ns of the laser drive. With CO_2 or He-H fills, LASNEX yields a similar T_e evolution, albeit with the expected lower n_e . For He and He-H only, LASNEX also shows a strong converging shock emanating from the domelike high-pressure LEH windows.

In inhomogeneous plasmas, the possible SBS gain length is usually controlled by the plasma-flow scale length L_v along the interaction beam [17], $L_v \equiv c_s / (\nabla v_p \cdot \hat{k}_0)$, where the ion acoustic speed is c_s (cm/s) = $3.1 \times 10^7 \sqrt{Z[T_e \text{ (keV)}] / A}$ and the atomic weight is A . From Fig. 1 (right) we infer $L_v \approx 1\text{--}3$ mm for the Nova hohlraum, comparable to $L_v \approx 6$ mm for NIF conditions (Fig. 2 in [4]). For He and He-H, LASNEX shows that the window-induced shock reduces L_v and increases T_i . With lower L_v , higher T_i , and lower n_e , we expect greatly reduced SBS gain in He and He-H hohlraums, which is borne out by our results.

The evolution of the radiation temperature T_r has been measured with Dante, an array of filtered x ray diodes [18]. Peak T_r in four neopentane hohlraums measured 202 ± 5 eV. LASNEX quantitatively models the T_r evolution well. Thus we infer from LASNEX modeling that the drive beams traverse the fill plasma at nearly full power and get absorbed mostly in the gold wall, rather than scattering and leaving the hohlraum.

T_e has been diagnosed radially at the hohlraum mid-plane by Cr-Ti isoelectronic x ray spectroscopy [19] with

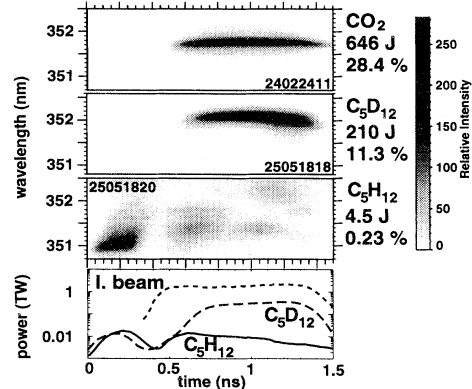


FIG. 2. Spectra of backscatter into the interaction-beam cone ($f/4.3$) are shown for three typical shots. The gas fills, backscattered energies (excluding scatter from other beams), and corresponding reflectivities are indicated. The interaction beam and reflected SBS powers for shots 25051818 and 25051820 are plotted in the bottom graph.

time-resolving Bragg-diffraction spectrometers [20]. We place within the hohlraum a 6- μ m-diam. graphite fiber previously co-sputtered with equal parts of Cr and Ti to a thickness of 0.1 μ m [19,20]. LASNEX simulations of hohlraums with fibers show very rapid T_e equilibration of Cr and Ti with the surrounding plasma. The measured $T_e = 3.0 \pm 0.5$ keV throughout the volume just inside the wall is consistent with LASNEX.

There is evidence that the n_e profiles are not as uniform as LASNEX predicts. The neopentane simulation shows at time 1 ns (see Fig. 1) where the beams cross the midplane that $n_e \approx 0.10\text{--}0.15n_c$, rising to $0.25n_c$ after 1.2 ns due to shocks arriving from the window plasma. Density diagnostics include narrowly collimated detection at 104° from \hat{k}_0 of stimulated Raman scatter (SRS) and $(3/2)\omega$ emission from two-plasmon decay. These measurements indicate the presence of $n_c/4$ at the mid-plane (± 0.1 mm) within the interaction beam as early as 0.7–1 ns [21]. Strong SRS emission corresponding to $n_e/n_c = 0.03\text{--}0.15$ is also observed [21], perhaps showing density depletion from self-focusing.

III. INTERACTION BEAM AND DIAGNOSTIC

The 351-nm interaction beam (No. 7) has a random-phase plate to spatially smooth the beam [22]. The resulting beam has hot spots of average width = $f\lambda$ and length = $7f^2\lambda$, where most SBS gain is expected to occur [15]. The pulse shape is a 1-ns square pulse turned on at time 0.4 ns, which allows interaction with a preheated plasma. Interaction-beam intensities quoted in this paper are those at the peak of the average-intensity envelope, not those of individual speckles.

The backscatter within the cone of the interaction beam is collimated by the focusing lens, and a known fraction passes through the last laser-turning mirror. The full-aperture backscatter station (FABS) diagnostic is located behind this mirror. The backscattered beam is attenuated, filtered to select the SBS frequency band, and focused onto both time-integrating calorimeters and

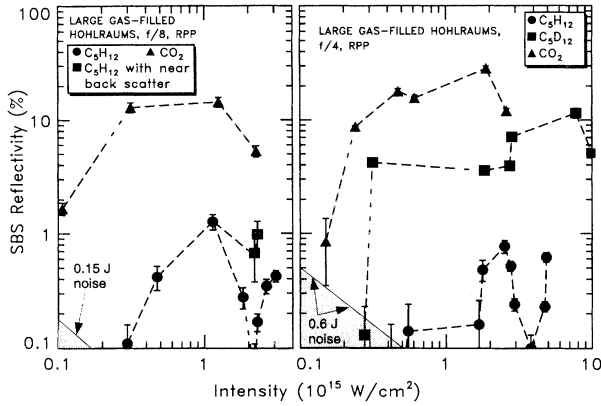


FIG. 3. SBS reflectivity (into the interaction-beam cone) from gas-filled hohlraums is plotted vs beam intensity.

a spectrometer coupled to a streak camera. The system is calibrated by firing the beam into a calibrated spherical fused-silica optic and detecting the known reflection.

IV. BACKSCATTER RESULTS

The SBS into FABS, shown in Fig. 2, is redshifted, as expected from the predicted subsonic plasmas (Fig. 1). There is modest heater-beam scatter into the interaction-beam cone, particularly before the interaction beam turns on (see Fig. 2). This spurious scatter is quantified with “null” shots, where the lens is focused but the beam is not fired. For an $f/4.3$ cone, this scatter is 2.9 ± 0.6 J for C_5H_{12} , C_5D_{12} and CO_2 and 0.9 ± 0.2 for He and He-H. It is about 4 times smaller for $f/8$. The 0.6-J uncertainty drives the noise floor shown in Fig. 3 right.

FABS SBS reflectivity data (ratio of reflected to incident energy of the interaction beam) are shown in Fig. 3, where the heater-beam contribution has been subtracted. The figure shows a dramatic effect of the ion species on the SBS reflectivity. The reflectivity appears to correlate inversely with Landau damping rates of the SBS ion wave. For Nova conditions ($T_i/T_e \approx 0.2$), the estimated Landau-damping rates normalized to the ion acoustic frequency (ν_i/ω_i) for He-H, C_5H_{12} , C_5D_{12} , He, and CO_2 are 0.35, 0.25, 0.15, 0.01, and 0.01 [23,24]. It is noteworthy that NIF designs now rely on a He-H mixture for SBS control instead of He alone. This is validated by comparing our reflectivity data from He with those from He-H. Remember that He and He-H reflectivities should not be compared to the others. Our He and He-H hohlraums should have lower SBS gain (lower n_e and L_w , higher T_i), as discussed above. In the $(1-3.5) \times 10^{15}$ W/cm² range, direct backscatter is $0.26 \pm 0.06\%$ for He while only $0.04 \pm 0.02\%$ for He-H. The comparisons between C_5H_{12} and C_5D_{12} , and between He and He-H, rule out n_e or T_e variability as the culprit for saturation variability.

A strong dependence of SBS reflectivity on ion damping rate is surprising since even at $\nu_i/\omega_i \approx 1$, the calculated linear SBS gain with the average (let alone hot-spot) laser intensity in these plasmas is enough to reflect most of the light [e.g., Eq. 1 in Ref. [4]]. So even with

enhanced damping from anomalous ion heating due to trapping [25], high reflectivities should still be observed.

The dips in direct backscatter with neopentane (Fig. 3) at $(2-3) \times 10^{15}$ W/cm² are due to the centroid of the SBS backscatter shifting away from the beam-cone axis by a few degrees. This novel effect has been diagnosed with the near backscatter imager (NBI) diagnostic. It monitors the SBS fluence from 162° from \hat{k}_0 to just outside the interaction-beam cone at $\approx 173^\circ$. The NBI is a calibrated Al diffuser ring, placed against the inside wall of the target chamber, which is imaged by a filtered, absolutely calibrated camera. Figure. 3, left panel, shows that when the net NBI contribution (after null-shot subtraction) is added, the reflectivity from C_5H_{12} does not really dip, but remains around a saturated value. SBS at $60^\circ-150^\circ$ from \hat{k}_0 is detected with the oblique scatter array (OSA) diagnostic [26], an array of filtered absolutely calibrated photodiodes and co-located fiber optics coupled to a streak camera for time resolution. SBS fluences at these angles (hundreds of J/sr) appear to be mostly due to the heater beams. Further details of oblique scatter and the observed backscatter angular shift are the subject of future papers.

Since the beam divergence within the target is not negligible for $f/4.3$, there is uncertainty in calculating the relevant vacuum laser intensity for Fig. 3. To resolve this, we note that, given $T_e = 3$ keV, the scattered-light redshift should be 0.9 nm (neglecting any plasma-flow Doppler shift). Combining observed shifts with plasma-flow modeling (see Fig. 1, right), the SBS location within the hohlraum and the correct intensity can be estimated. The $f/4.3$ interaction beam was focused either near the midplane or near the LEH (at the crossing of the axis). When focused at the midplane, the relative intensity at the wall and at the LEH is about 0.65 of the midplane value. When focused at the LEH, intensities (relative to peak) are 0.65 at the midplane and 0.3 at the wall. For the $f/8$ beam, always focused at the midplane, the LEH and wall intensities are 0.8 of the midplane value. In Fig. 3, LEH intensities were used for C_5H_{12} and CO_2 for consistency with the observed smallish redshifts late in time (see Fig. 2). For C_5D_{12} , large redshifts indicate using the midplane intensity in Fig. 3.

The shapes of the reflectivity-intensity curves (Fig. 3 including near backscatter for C_5H_{12}) are like the theoretical prediction in Ref. [15], Fig. 1. SBS turns on at an onset critical intensity I_c and saturates slightly above I_c . With increased damping, the calculated I_c increases because stronger drive is necessary to get significant SBS gain [15]. This is validated by the higher I_c observed as the fill is changed from CO_2 to C_5D_{12} and to C_5H_{12} . The Ref. [15] model is strictly valid only in the strong-damping limit. Extension to CO_2 is thus uncertain.

V. DISCUSSION

As predicted [15], the observed C_5H_{12} value of $I_c \approx 3 \times 10^{14}$ W/cm² for $f/8$ in Fig. 3 is lower than the $I_c \approx 1.5 \times 10^{15}$ W/cm² for $f/4.3$. The longer $f/8$ hot spots require less intensity to achieve the same SBS gain. But

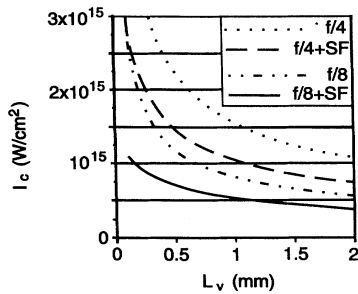


FIG. 4. Calculated critical intensities for $f/4$ and $f/8$, with and without self-focusing included, are plotted vs L_v for $\nu_i/\omega_i = 0.25$, $n_e/n_c = 0.1$, and $T_e = 3$ keV, i.e., C_5H_{12} .

both values are lower than those calculated using Eq. (16) in Ref. [15]. A better calculation includes the effects of nascent self-focusing (SF), which modestly increases hot-spot intensity, which in turn increases SBS, finite L_v , and multiple ranks of hot spots [27]. Both I_c estimates are compared in Fig. 4. For a nominal $L_v \approx 1$ mm, the calculated I_c including SF for both f numbers (solid and dashed lines) are reasonably close to the observed I_c .

Detailed comparison of our data to the model in Ref. [15] beyond the existence and value of I_c is not valid for two reasons. First, the calculation assumes thermal levels for the seed from which SBS grows. Seed levels in Nova plasmas appear to be much larger. Second, the only saturation mechanism in the model is pump depletion, clearly unrealistic given our data. These two effects do not affect the predicted I_c values, but they change the noise floor and the saturated value of the reflectivity.

VI. SUMMARY

In conclusion, Nova hohlraums with conditions approaching those expected within ignition hohlraums have been designed and characterized. Conditions have been varied to better understand SBS. SBS reflectivity from the most ignitionlike plasmas (C_5H_{12}) is small. As the laser intensity is increased, the SBS reflectivity increases sharply as an onset intensity I_c is reached, and saturates slightly above I_c . This feature is in agreement with theory [15]. The dependencies of I_c on f /number and on acoustic damping also agree with theory (Fig. 4 and Ref. [15]). The saturation level, which strongly decreases with increased estimated damping rate, is not understood. Finally, we observe a deflection of the backscatter out of the beam cone at a certain intensity. A possible explanation, related to cross-beam plasma flow and filamentation, is the subject of a future manuscript.

ACKNOWLEDGMENTS

The authors wish to thank the Nova operations team and the Los Alamos technicians supporting Nova. We acknowledge many useful discussions with D. DuBois and B. Bezzerides of LANL, and with R. Berger, R. Kauffman (a strong advocate of hohlraum SBS experiments), J. Kilkenny, J. Lindl, B. MacGowan, L. Powers, and R. Turner of LLNL. M. Salazar (LANL) and G. Stone (LLNL) did copious and dedicated work supporting target gas-fill operations. J. Miller (LLNL) did the optics design and calibration of the FABS diagnostic. This work was supported by the U.S. Department of Energy.

- [1] J. H. Nuckolls, L. Wood, A. R. Thiessen, and G. B. Zimmerman, *Nature* **239**, 139 (1972).
- [2] J. D. Lindl, R. L. McCrory, and E. M. Campbell, *Phys. Today* **45** (9), 32 (1992).
- [3] S. W. Haan *et al.*, *Phys. Plasmas* **2**, 2480 (1995).
- [4] L. V. Powers *et al.*, *Phys. Plasmas* **2**, 2473 (1995).
- [5] L. M. Gorbunov, *Zh. Eksp. Teor. Fiz.* **55**, 2298 (1968) [*Sov. Phys. JETP* **28**, 1220 (1969)].
- [6] K. A. Tanaka *et al.*, *Phys. Fluids* **27**, 2960 (1984).
- [7] P. E. Young *et al.*, *Phys. Fluids B* **2**, 1907 (1990).
- [8] R. A. Haas *et al.*, *Phys. Fluids* **20**, 322 (1977).
- [9] B. J. MacGowan *et al.*, in *Proceedings of the 15th International Conference on Plasma Physics and Controlled Nuclear Fusion Research* (International Atomic Energy Agency, Vienna, 1994), p. 16.
- [10] D. M. Villeneuve, H. A. Baldis, and J. E. Bernard, *Phys. Rev. Lett.* **59**, 1585 (1987).
- [11] H. A. Baldis *et al.*, *Phys. Rev. Lett.* **62**, 2829 (1989).
- [12] K. A. Tanaka *et al.*, *Phys. Rev. Lett.* **58**, 33 (1987).
- [13] L. V. Powers *et al.*, *Phys. Rev. Lett.* **74**, 2957 (1995).
- [14] E. M. Campbell, *Rev. Sci. Instrum.* **57**, 2101 (1986).
- [15] H. A. Rose and D. F. DuBois, *Phys. Rev. Lett.* **72**, 2883 (1994).
- [16] G. Zimmerman and W. Kruer, *Comments Plasma Phys. Controlled Fusion* **2**, 51 (1975).
- [17] C. S. Liu, M. N. Rosenbluth, and R. B. White, *Phys. Fluids* **17**, 1211 (1974).
- [18] H. N. Kornblum, R. L. Kauffman, and J. A. Smith, *Rev. Sci. Instrum.* **57**, 2179 (1986).
- [19] R. S. Marjoribanks, F. Budnik, G. Kulcsár, and L. Zhao, *Rev. Sci. Instrum.* **66**, 683 (1995).
- [20] B. H. Failor, R. Hockaday, and W. W. Hsing, *Rev. Sci. Instrum.* **66**, 767 (1995).
- [21] J. A. Cobble *et al.*, *Rev. Sci. Instrum.* **66**, 4202 (1995).
- [22] S. M. Dixit *et al.*, *Appl. Opt.* **32**, 2543 (1993).
- [23] H. X. Vu, J. M. Wallace, and B. Bezzerides, *Phys. Plasmas* **1**, 3542 (1994).
- [24] E. A. Williams *et al.*, *Phys. Plasmas* **2**, 129 (1995).
- [25] W. L. Kruer, *Phys. Fluids* **23**, 1273 (1980).
- [26] J. C. Fernández *et al.*, *Rev. Sci. Instrum.* **66**, 626 (1995).
- [27] H. A. Rose, *Phys. Plasmas* **2**, 2216 (1995).

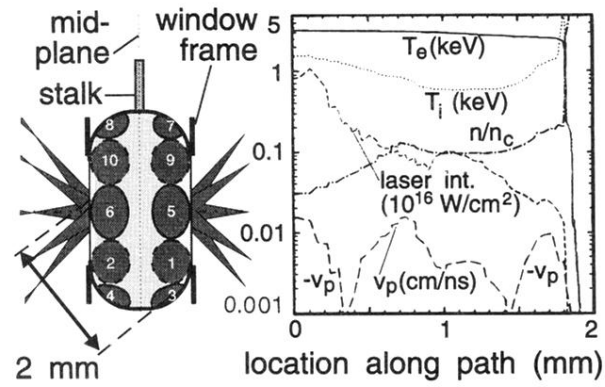


FIG. 1. Left: The gas-filled hohlraum is illustrated. The footprints of the ten Nova beams incident on the inner wall are indicated (those on the far wall have a dashed outline). Right: Calculated profiles within the hohlraum along a beam path (starting at the LEH) are plotted for time 1 ns.

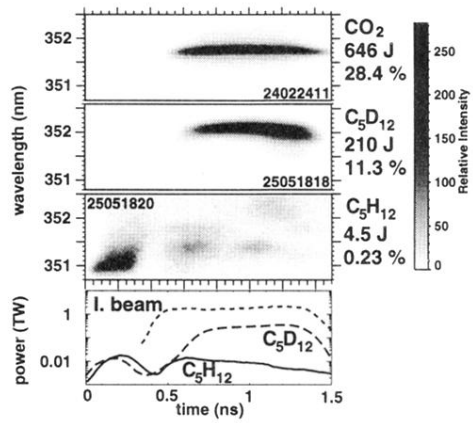


FIG. 2. Spectra of backscatter into the interaction-beam cone ($f/4.3$) are shown for three typical shots. The gas fills, backscattered energies (excluding scatter from other beams), and corresponding reflectivities are indicated. The interaction beam and reflected SBS powers for shots 25051818 and 25051820 are plotted in the bottom graph.